Journal of Hazardous Materials 174 (2010) 707–713

Contents lists available at ScienceDirect

Journal of Hazardous Materials

journal homepage: www.elsevier.com/locate/jhazmat

Photocatalytic activity of TiO_2/SiO_2 systems

M. Bellardita[a], M. Addamo[a], A. Di Paola[a], G. Marcì[a], L. Palmisano[a,*], L. Cassar[b], M. Borsa[c]

[a] "Schiavello-Grillone" Photocatalysis Group, Dipartimento di Ingegneria Chimica dei Processi e dei Materiali, Università di Palermo, Viale delle Scienze, 90128 Palermo,Italy
[b] Italcementi S.p.A., San Donato Milanese, Italy
[c] Italcementi S.p.A, Brindisi, Italy

ARTICLE INFO

Article history:
Received 17 June 2009
Received in revised form 8 September 2009
Accepted 21 September 2009
Available online 24 September 2009

Keywords:
Photocatalysis
TiO_2/SiO_2 systems
Gas–solid reactions
Photocatalytic cement
Urban pollution

ABSTRACT

Silica-supported TiO_2 powders were synthesized by a wet method under mild conditions. The aim of the work was the preparation of TiO_2/SiO_2 additives for photocatalytic cements. Three types of commercial SiO_2 were used as supports: Cabot, Axim and Fly Ash. Cabot silica was ultra-pure whereas the other two silica contained different percentages of various oxides. The TiO_2/SiO_2 samples, denoted TiO_2/Cabot, TiO_2/Axim and TiO_2/Fly Ash, were prepared by boiling suspensions obtained by addition of silica to a solution of $TiCl_4$ in water (volume ratio 1:10). The photocatalytic activity was evaluated in a gas–solid system both in batch and in continuous reactors using 2-propanol as probe molecule. SEM-EDX analysis revealed that titanium dioxide was quantitatively deposited on silica. TiO_2/Axim and TiO_2/Fly Ash were scarcely active whereas a good photoactivity was exhibited by the TiO_2/Cabot sample both in the batch and in the continuous system. Consequently only the last sample was tested for both NO_x abatement and for 4-nitrophenol photodegradation in a liquid–solid system.

1. Introduction

Heterogeneous photocatalysis [1–4] has shown a high efficiency in the photooxidation of many organic pollutants present in air [5,6] or in liquid effluents [7–9]. It allows pollution abatement under mild condition (room temperature and pressure) and avoids the use of noxious metal species often present in the classical catalytic depollution processes. Among various semiconductors, TiO_2 is the most used photocatalyst because of its high photocatalytic activity, non-toxicity, low cost and photochemical stability in the reaction conditions [10–12].

A good photocatalyst should possess a high specific surface area available for the adsorption and decomposition of the organic pollutants. A simple method to increase the adsorption capacity of TiO_2 is the use of a support with large surface area and high porosity. Siliceous materials are often employed as supports because they are chemically inert, transparent to the UV radiation and with a high specific surface area.

SiO_2-supported TiO_2 materials have been extensively used as catalysts for a wide variety of reactions because their physicochemical properties are superior than those of the single oxides [13]. The properties of the TiO_2/SiO_2 systems depend on the synthesis conditions and on the degree of interaction between the two oxides.

Many works have been concerned with the application of TiO_2/SiO_2 materials in photocatalytic processes [14–26]. TiO_2/SiO_2 powders have been often prepared to make easier the separation of the catalyst after the photocatalytic reaction but these photocatalysts are commonly less active than bare TiO_2. Only few works reported the preparation of TiO_2/SiO_2 samples more efficient than TiO_2 alone [27–29]. The enhancement of photoactivity was attributed to the increased adsorption of organic substrate, to the increased specific surface area of the supported TiO_2, to the interaction between titanium dioxide and silica and also to the different structure of surface titanate from that of bulk titania.

Silica gel-supported TiO_2 particles have been studied for the photodegradation of dyes that are the main pollutants produced from the textile industries [19,25,26]. Titania–silica materials with photocatalytic properties could be incorporated as additives into concrete matrices for self-cleaning building surfaces or to eliminate noxious pollutants present in the urban environment.

Various procedures have been employed to synthesize titania–silica materials: sol–gel hydrolysis [15,27,28,30], grafting of titanium alkoxides on the SiO_2 surface [31,32], coprecipitation [33], impregnation [34], chemical vapor deposition [35].

In last years there is an increasing interest in the control of urban pollution (especially the NO_x and VOCs level) by using construction materials containing TiO_2 that do not modify the aesthetic characteristics of the structures. In particular cementitious materials (e.g. paints, asphalts, paving blocks) containing TiO_2 have been recently produced and applied on several buildings and other structures.

* Corresponding author. Tel.: +39 091 238 63746; fax: +39 091 702 5020.
E-mail address: palmisano@dicpm.unipa.it (L. Palmisano).

0304-3894/$ – see front matter © 2009 Elsevier B.V. All rights reserved.
doi:10.1016/j.jhazmat.2009.09.108

In this work we report the preparation and the characterization of TiO_2/SiO_2 powders obtained by supporting TiO_2 on three different types of commercial SiO_2. The aim of the work was the synthesis of TiO_2/SiO_2 systems that could be employed for the production of photocatalytic cements. The TiO_2/SiO_2 samples were prepared by a wet method under mild conditions using $TiCl_4$ as the TiO_2 precursor. The photocatalytic activity of the samples was evaluated following the oxidation of 2-propanol in gas–solid regimen both in batch and in continuous reactors. The best catalyst was also tested for the abatement of NO_x and for the degradation of 4-nitrophenol.

2. Experimental

2.1. Preparation of the samples

Three different types of commercial SiO_2 were used as supports: Cabot, Axim and Fly Ash. Cabot silica was ultra-pure whereas the other two silicas, derived from the combustion of minerals (quartzite), contained different percentages of various oxides as CaO, MgO, Al_2O_3, Fe_2O_3, K_2O, Na_2O.

Titanium tetrachloride (Fluka 98%) was used without any further purification. $TiCl_4$ was slowly added to distilled water (volume ratio 1:10) at room temperature. The hydrolysis reaction was highly exothermic and produced high quantities of fumes of HCl. After ca. 10 h of continuous stirring a clear solution was obtained [36].

10 g of silica (Cabot, Axym or Fly Ash) were added to 110 mL of the $TiCl_4$ solution and the obtained suspension was boiled for 2 h. Water was continuously added to refill the evaporated quantity. The final suspension was dried in a rotary evaporator. The samples were denoted TiO_2/Cabot, TiO_2/Axim and TiO_2/Fly Ash, respectively. The weight percentage of TiO_2 contained in all the samples was 42%.

2.2. Characterization of the samples

XRD patterns of the powders were recorded at room temperature by a Philips powder diffractometer using the Cu Kα radiation and 2θ scan rate of $2^\circ\,min^{-1}$. The specific surface areas (SSA's) of the powders were determined in a Flow Sorb 2300 apparatus (Micromeritics) by using the single-point BET method. The samples were degassed for 30 min at 250 °C prior to the measurement.

Scanning electron microscopy observations were obtained using a Philips XL30 ESEM microscope instrument, operating at 30 kV on specimens upon which a thin layer of gold was deposited. An electron microprobe used in an energy dispersive mode (EDX) was employed to obtain information on the content of titanium and silicon in the samples. Visible–ultraviolet spectra were obtained by diffuse reflectance spectroscopy by using a Shimadzu UV-2401 PC instrument. $BaSO_4$ was the reference sample and the spectra were recorded in the range 200–600 nm.

2.3. Photoreactivity experiments

The photoreactivity of the various samples was evaluated in gas–solid regimen in a cylindrical Pyrex batch photoreactor ($V = 0.9\,dm^3$). Thin layers of the powders (ca. 0.5 g) were prepared by spreading the slurries obtained by mixing the powders with water on glass supports that were subsequently dried at 60 °C for 30 min. The samples were irradiated from the top by a UV 500 W medium pressure Hg lamp. A water filter was placed between the lamp and the photoreactor to cut the infrared radiation. The irradiance at the powder surface was $1.3\,mW\,cm^{-2}$. Before starting the photodegradation reaction the reactor was purged and saturated with O_2. Subsequently, fixed amounts of 2-propanol were directly injected into the reaction chamber and the lamp was switched on. 0.5 cm^3 of the gaseous mixture were withdrawn at different irradiation times using a gas tight syringe and analyzed by gas chromatography.

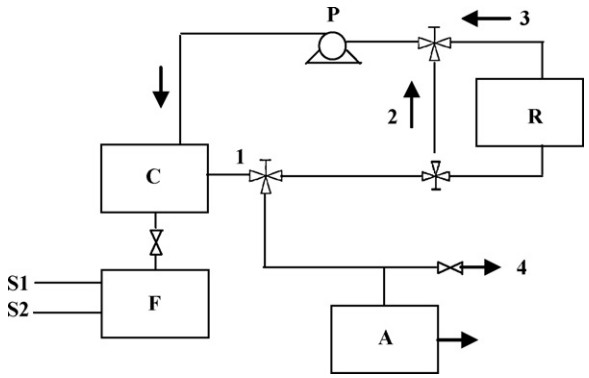

Fig. 1. Experimental setup for NO_x measurements. In this scheme, letters indicate: NO_x ($NO + NO_2$); source (S_1); pure air (S_2); flux meter (F); gas mixing chamber (C); reaction chamber (R); NO_x analyzer (A); membrane pump (P).

The photodegradation of 2-propanol was also carried out in a continuous cylindrical Pyrex gas–solid reactor ($V = 1.5\,dm^3$). The powders were mixed with water, spread on the walls of the reactor and dried at 60 °C for 30 min. A 500 W medium pressure Hg lamp was used for the irradiation of the catalyst. The irradiance at the film surface was $17\,mW\,cm^{-2}$. The reacting mixture obtained by bubbling O_2 in an aqueous solution of 2-propanol was fluxed into the reactor before irradiation and throughout the duration of the run. When the concentration of the substrate was the same in the inlet and in the outlet stream the lamp was switched on.

2-Propanol and propanone concentrations were measured by a GC-17A Shimadzu gas chromatograph equipped with a HP-1 column and a flame ionization detector. CO_2 was detected by a HP 6890 Series GC System equipped with a packed column GC 60/80 Carboxen-1000 and a thermal conductivity detector (TCD). Helium was used as the carrier gas.

The activity of the sample that yielded the best photocatalytic responses was also evaluated by two test reactions: NO_x abatement and 4-nitrophenol degradation.

4-Nitrophenol was photodegraded in a liquid–solid batch reactor using a 125 W medium pressure Hg lamp (Helios Italquartz, Italy). The irradiance was $10.8\,mW\,cm^{-2}$. Samples of 5 cm^3 were withdrawn at fixed intervals of time with a syringe and the catalyst was removed from the solution by filtration through 0.1 μm PTFE membranes (Whatman). The quantitative determination of 4-nitrophenol was performed by measuring its absorption at 315 nm. The intermediates obtained from 4-nitrophenol photodegradation did not interfere according also to the results of other authors [37,38].

As far as the NO_x abatement is concerned [39], the experimental set up is reported in Fig. 1. The scheme illustrates a batch recirculation system where a certain concentration of NO_x was first introduced with air in a large volume chamber (C, 20 L) and after mixing (re-circulation via routes 1–2), the test gaseous mixture was allowed to circulate ($4.5\,L\,min^{-1}$) through the reaction chamber (R) (routes 1–3) in the dark, and analyzed at established time intervals (routes 1–4). For the photocatalytic tests, the catalyst sample was positioned in the reaction chamber R which was provided with an optical window for illumination. An Osram Vitalux lamp was used for irradiation. The irradiance was $15\,mW\,cm^{-2}$. Humidity was controlled at 50–60%. The NO_x concentration was detected by a chemiluminescence analytical method by a Nitrogen Oxides Analyzer Environment SA AC32M instrument [40].

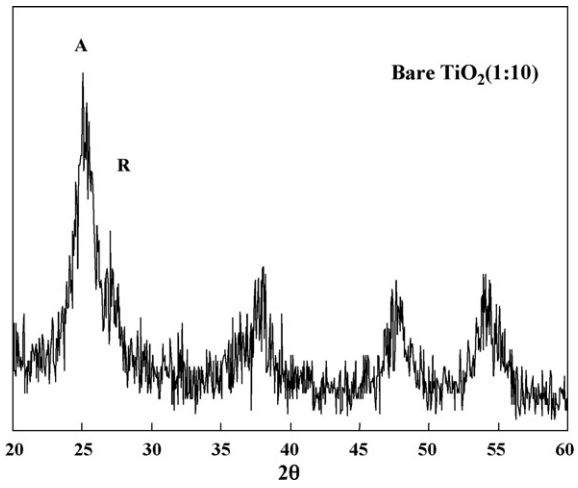

Fig. 2. XRD pattern of the bare TiO_2 obtained by boiling of a 1:10 $TiCl_4/H_2O$ mixture for 2 h. A: Anatase, R: rutile.

3. Results and discussion

3.1. Characterization

Efficient TiO_2 photocatalysts can be prepared by controlling the hydrolysis of $TiCl_4$ in pure water [36]. Fig. 2 shows the X-ray diffraction pattern of the solid obtained by drying at room temperature the suspension formed after boiling of a 1:10 $TiCl_4/H_2O$ mixture for 2 h. The diffractogram reveals the presence of a badly crystallized anatase phase and of a small amount of rutile.

Fig. 3a shows the XRD patterns of bare Cabot silica and of the TiO_2/Cabot sample. The ultra-pure silica was completely amorphous whereas TiO_2/Cabot contained anatase and traces of rutile. The peaks were broad indicating a very small size of badly crystallized grains due to the low temperature of preparation of the samples.

Fig. 3b and c shows the diffractograms of the powders prepared by supporting TiO_2 onto the other two types of silica. All the peaks present in the X-ray patterns of the bare samples are ascribable to the impurities contained in the starting materials. The main peak of anatase was clearly detected in the diffractograms of both TiO_2/SiO_2 samples.

Table 1 reports the specific surface areas of the tree types of commercial silica and of all the supported samples. Cabot silica revealed a very high SSA value whereas that of the sample obtained depositing TiO_2 onto this type of silica was slightly lower than that measured for the support.

The specific surface areas of Axim and Fly Ash silicas were lower than that of the Cabot powder but the SSA values of the corresponding TiO_2/SiO_2 samples were higher than those of the bare supports.

SEM-EDX analyses were employed to study the morphology of the particles and the homogeneity of the TiO_2 distribution onto the support. In Fig. 4 the SEM images of the studied samples are reported. From the images relative to the samples TiO_2/SiO_2 it can

Table 1
Specific surface area of the various samples.

Sample	SSA ($m^2\ g^{-1}$)
Cabot silica (SiO_2: 99%)	191
TiO_2/Cabot	177
Axim silica (SiO_2: 90–95%)	29
TiO_2/Axim	49
Fly Ash silica (SiO_2: 45–50%)	4.7
TiO_2/Fly Ash	29

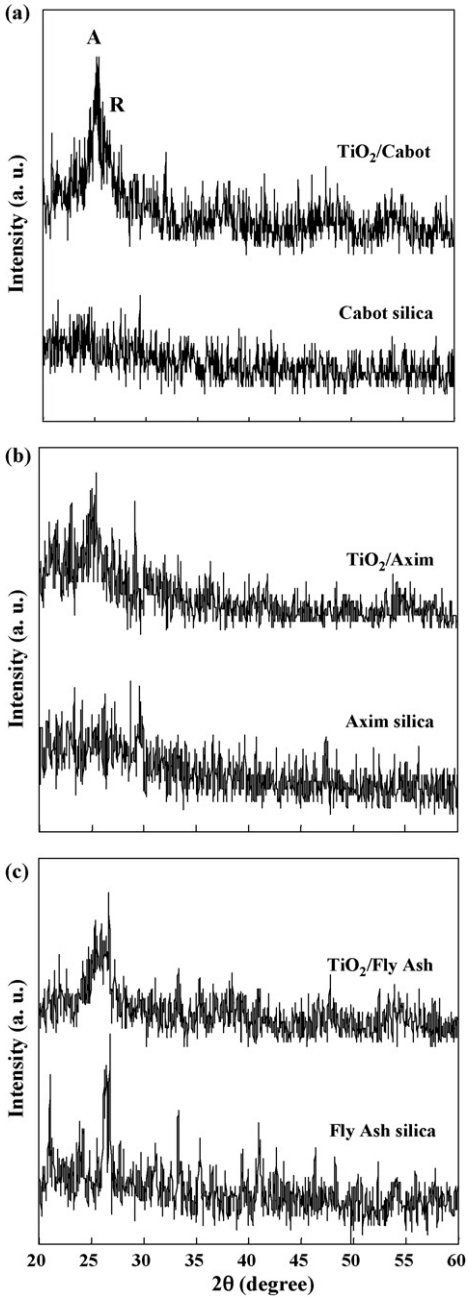

Fig. 3. XRD patterns of the bare silica and TiO_2/SiO_2 samples. A: Anatase, R: rutile.

be noticed that the silica particles worked as nucleation centres for the precipitation of TiO_2, independently of the silica type. The morphology of the TiO_2/SiO_2 samples was very different from that of the corresponding bare support.

The micrographs of the bare Cabot silica and of the TiO_2/Cabot sample are shown in Fig. 4a and b, respectively. Cabot silica consisted of primary particles whose dimensions were smaller than 100 nm. After the deposition of TiO_2, nanostructured agglomerates of irregular shape were obtained. The average sizes of the TiO_2/SiO_2 primary particles were bigger than those of bare silica and ranged between 100 and 200 nm. Pore clogging obstruction by the TiO_2 particles justifies the reduction of specific surface area in the TiO_2/Cabot sample.

Axim silica (Fig. 4c) consisted of agglomerates of primary particles bigger than those of Cabot silica. The particles presented uneven shapes and dimensions. As shown by the micrograph of

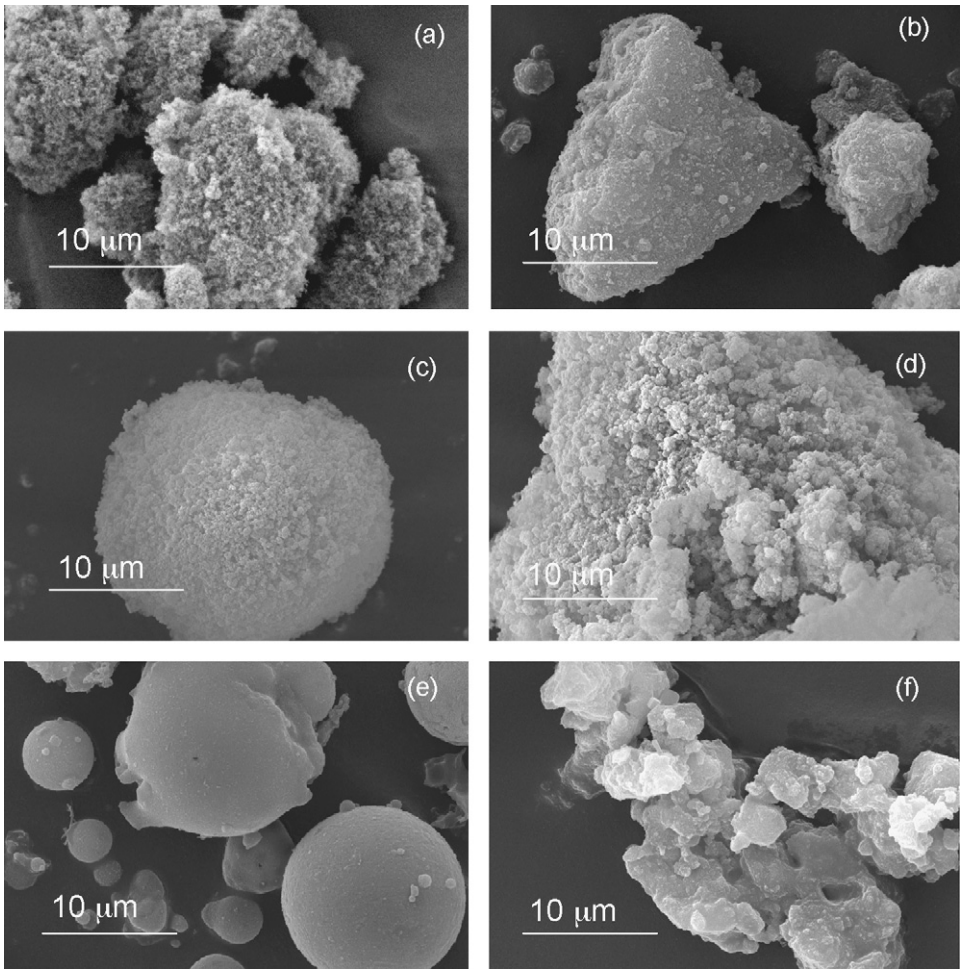

Fig. 4. SEM micrographs of the various samples: (a) Cabot silica; (b) TiO_2/Cabot; (c) Axim silica; (d) TiO_2/Axim; (e) Fly Ash silica; (f) TiO_2/Fly Ash.

the TiO_2/Axim sample (Fig. 4d), when TiO_2 was deposited onto the Axim silica the particles resulted larger and the surface became rougher.

Bare Fly Ash silica (Fig. 4e) revealed a different morphology. This type of silica was formed by very compact sphere-shaped particles. The comparison with the micrograph of the TiO_2/Fly Ash sample (Fig. 4f) indicates that TiO_2 precipitated onto silica particles incorporating various particles.

The increased surface area of TiO_2/Axim and TiO_2/Fly Ash with respect to that of the corresponding silicas could be ascribable to the highest roughness of the deposited TiO_2.

EDX measurements confirmed that TiO_2 was completely deposited on the silica supports since no particles constituted only by titania or silica were found. All the TiO_2/SiO_2 samples revealed a more or less homogeneous titanium layer onto the various particles. Both the average global percentages of Ti and Si and those of several zones of the samples were determined. The local values presented only a scattering of ±15% with respect to the average global ones.

Fig. 5 shows the diffuse UV–vis reflectance spectra of the three TiO_2/SiO_2 materials and of a pure TiO_2 sample obtained following the same synthetic procedure in the absence of silica. The high absorption exhibited in the visible region by TiO_2/Axim and TiO_2/Fly Ash is attributable to the presence of the various species contained in the support. This means that the features of the spectra of these two samples are prevalently due to the contribution of the supports (spectra not reported for the sake of clarity), whose colour is greyish.

By assuming TiO_2 as an indirect semiconductor [41], the band gap energy, E_g, of the various samples was determined from the tangent line in the plots of the modified Kubelka–Munk function $[F(R'_\infty)h\nu]^{1/2}$ versus the energy of the exciting light [42]. The E_g values estimated for TiO_2/Cabot (3.02 eV) and TiO_2/Axim (2.98 eV) respectively, were very near to that of bare TiO_2 (3.00 eV). This result is in agreement with the EDX analysis indicating that TiO_2 covered the SiO_2 particles. Similar results are reported in the litera-

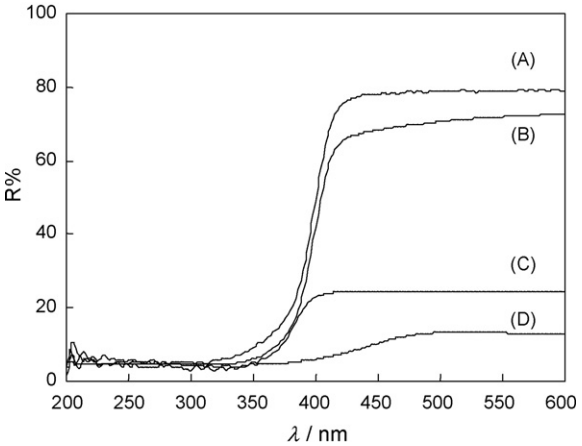

Fig. 5. Diffuse reflectance spectra of the samples: (A) TiO_2/Cabot; (B) bare TiO_2; (C) TiO_2/Axim; (D) TiO_2/Fly Ash.

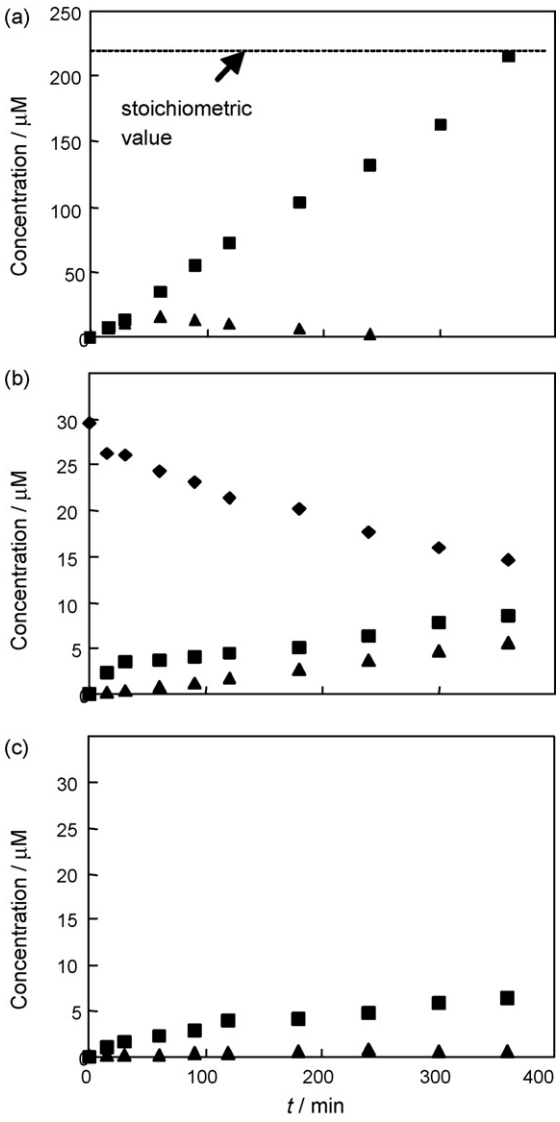

Fig. 6. Photocatalytic degradation of 2-propanol in the batch reactor in the presence of the samples: (a) TiO_2/Cabot; (b) TiO_2/Axim; (c) TiO_2/Fly Ash. (♦) 2-Propanol; (▲) propanone; (■) CO_2.

ture for silica-supported TiO_2 with high titania contents. Anderson and Bard found that when the TiO_2 domains in TiO_2/SiO_2 materials were sufficiently large (>3 nm), the E_g values were equal or very close to the bulk value of TiO_2 [27]. van Grieken et al., who studied silica-supported materials with titania contents up to 60 wt.%, found a blue shift of the band gap absorption edge of all the supported samples with respect to that of pure bulk anatase [15]. The determination of the E_g of TiO_2/Fly Ash is obviously meaningless since the features of the spectrum are prevalently due to the contribution of the various species contained in the support.

3.2. Photoreactivity results

Fig. 6 shows the photocatalytic results obtained in the batch reactor with the three TiO_2/SiO_2 samples. 2-Propanol was completely adsorbed onto the surface of the TiO_2/Cabot sample and it was absent in the gaseous phase. The amount of substrate introduced into the reactor corresponded to a 74 μM concentration. During the first minutes of irradiation (see Fig. 6a), 2-propanol was partially oxidized to propanone and CO_2. After about 100 min the measured amount of propanone decreased and the CO_2 concentration almost linearly increased. 2-Propanol was completely mineralized in about 6 h and the CO_2 concentration reached its stoichiometric value after the same time.

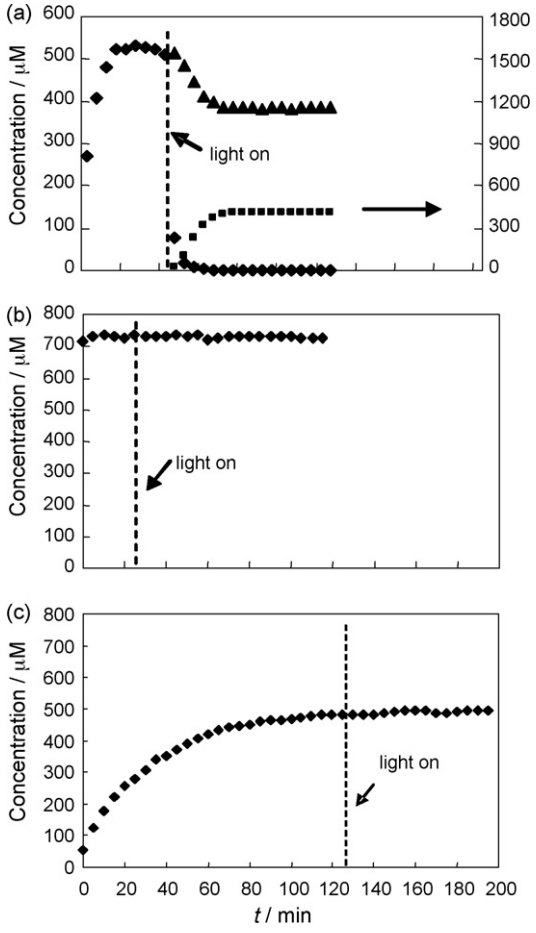

Fig. 7. Photocatalytic degradation of 2-propanol in a continuous reactor in the presence of the samples: (a) TiO_2/Cabot; (b) TiO_2/Axim; (c) TiO_2/Fly Ash. (♦) 2-Propanol; (▲) propanone; (■) CO_2.

It is worth noting that the photoactivity of both TiO_2/Axim and TiO_2/Fly Ash (see Fig. 6b and c) was significantly lower than that of TiO_2/Cabot, although the amount of 2-propanol introduced into the reactor was smaller (initial concentration: 30 μM).

2-Propanol was not adsorbed by the TiO_2/Axim sample and its concentration slowly decreased during the irradiation. After 6 h, the gaseous concentration of 2-propanol was about half the initial value while the amounts of propanone and CO_2 gradually increased. The carbon balance in the gaseous phase was not reached during the run probably because of (photo)adsorption of the 2-propanol intermediates on the catalyst surface.

Differently, 2-propanol was completely adsorbed onto the surface of the TiO_2/Fly Ash sample. The amount of propanone present in the gaseous phase during the irradiation was negligible indicating that either propanone remained adsorbed onto the surface or 2-propanol was directly mineralized to CO_2. Small amounts of CO_2 were formed.

Fig. 7 shows the results obtained in the continuous reactor. In the dark, 2-propanol was adsorbed by TiO_2/Cabot and the concentration increased until the saturation was reached. When the lamp was switched on, after a short transient, all entering 2-propanol was degraded and the concentration of propanone reached a constant value. 2-Propanol was not stoichiometrically transformed to propanone since CO_2 was contemporaneously generated.

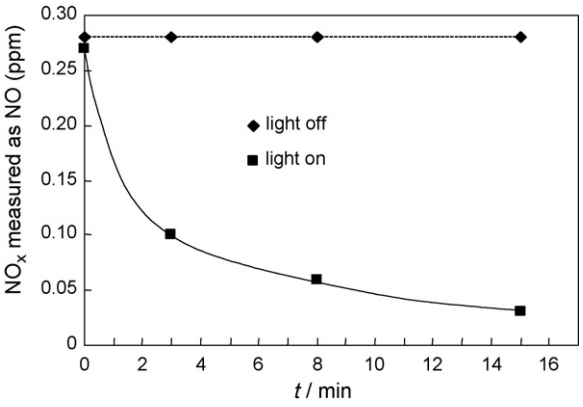

Fig. 8. NO_x abatement in the presence of TiO_2/Cabot sample.

TiO_2/Axim and TiO_2/Fly Ash did not exhibit any photocatalytic activity in continuous regimen. Under irradiation, the concentration of 2-propanol in the outlet stream was the same of that of the inlet stream and no propanone and/or CO_2 were detected. It is worth noting that in the presence of TiO_2/Axim, 2-propanol concentration remained constant in the dark, confirming that the substrate was not adsorbed onto the catalyst surface.

The highest photocatalytic activity exhibited by the TiO_2/Cabot sample (that revealed the highest SSA value) cannot be only justified by a larger adsorption capability of this material since 2-propanol was completely adsorbed also by TiO_2/Fly Ash. By taking into account that the percentage of TiO_2 contained in the three TiO_2/SiO_2 materials was equal, the scarce photoactivity of TiO_2/Axim and TiO_2/Fly Ash could be ascribable to the presence of other species, working as centres of recombination of the hole–electrons pairs. This effect was absent in the TiO_2/Cabot material because the commercial Cabot silica was very pure.

The active TiO_2/Cabot sample was also tested for the abatement of NO_x. Fig. 8 shows that the concentration of NO_x did not change under dark conditions. Instead more than about 90% of NO_x was abated after 15 min of treatment under irradiation.

Finally, TiO_2/Cabot was tested in liquid–solid regimen since dangerous pollutants can be dissolved in water or humidity present on the surface of cementitious structures. Fig. 9 shows the variation of 4-nitrophenol concentration versus irradiation time for a photocatalytic test carried out in the presence of TiO_2/Cabot. The initial concentration of 4-NP was 20 ppm and the substrate was completely degraded in about 4 h.

The photoactivity of TiO_2/Cabot remained practically the same when three photocatalytic runs were performed with the same sample both in the gas–solid and liquid–solid systems. The long-term stability of this material is encouraging for its possible employment in the cement industry.

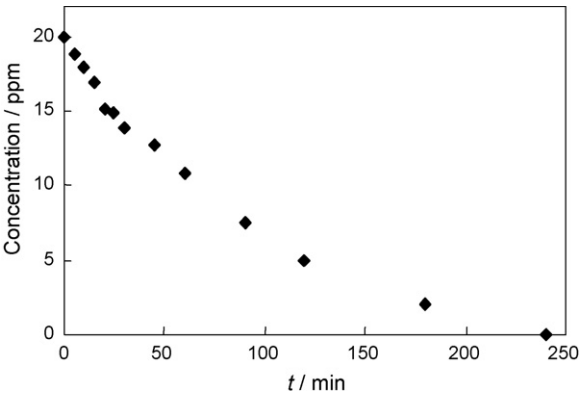

Fig. 9. Liquid–solid photocatalytic degradation of 4-nitrophenol in the presence of TiO_2/Cabot sample.

4. Conclusions

Different TiO_2/SiO_2 samples were prepared depositing TiO_2 onto three different types of silica by a wet method under mild conditions. In all the cases TiO_2 covered the silica particles indicating that they worked as nucleation centres for the TiO_2 particles independently of the kind of support. EDX analysis of the TiO_2/SiO_2 samples confirmed that all the TiO_2 was deposited onto the silica particles and revealed that the Ti/Si ratio was equal to the theoretical value calculated from the amounts of reactants. The good photocatalytic activity of the sample obtained by supporting TiO_2 on pure Cabot silica seems interesting for a possible employment of this material as additive for photocatalytic cements with the aim to abate noxious volatile organic compounds. The other two kinds of less expensive silicas (Axim and Fly Ash) are not suitable for photocatalytic applications.

Acknowledgments

The authors thank Prof. R. Amadelli and Dr. L. Samiolo, ISOF-CNR c/o Dipartimento di Chimica, Università di Ferrara, Italy, for the NO_x analysis.

References

[1] M. Schiavello (Ed.), Photocatalysis and Environment. Trends and Applications, Kluwer, Dordrecht, 1988.
[2] E. Pelizzetti, N. Serpone (Eds.), Photocatalysis: Fundamentals and Applications, John Wiley & Sons, New York, 1989.
[3] M.A. Fox, M. Dulay, Heterogeneous photocatalysis, Chem. Rev. 93 (1993) 341–357.
[4] M.R. Hoffmann, S.T. Martin, W. Choi, D.W. Bahnemann, Environmental applications of semiconductor photocatalysis, Chem. Rev. 95 (1995) 69–96.
[5] V. Augugliaro, S. Coluccia, V. Loddo, L. Marchese, G. Martra, L. Palmisano, M. Schiavello, Photocatalytic oxidation of gaseous toluene on anatase TiO_2 catalyst: mechanistic aspects and FT-IR investigation, Appl. Catal. B: Environ. 20 (1999) 15–27.
[6] J. Maira, J.M. Coronado, V. Augugliaro, K.L. Yeung, J.C. Conesa, J. Soria, Fourier transform infrared study of the performance of nanostructured TiO_2 particles for the photocatalytic oxidation of gaseous toluene, J. Catal. 202 (2001) 413–420.
[7] D.F. Ollis, H. Al-Ekabi (Eds.), Photocatalytic Purification and Treatment of Water and Air, Elsevier, Amsterdam, 1993.
[8] J.M. Herrmann, Active agents in heterogeneous photocatalysis: atomic oxygen species vs. OH radicals: related quantum yields, Helv. Chim. Acta 84 (2001) 2731–2750.
[9] V. Augugliaro, L. Palmisano, A. Sclafani, C. Minero, E. Pelizzetti, Photocatalytic degradation of phenol in aqueous titanium dioxide dispersions, Toxicol. Environ. Chem. 16 (1988) 89–109.
[10] A. Fujishima, T. Rao, D.A. Tryk, Titanium dioxide photocatalysis, J. Photochem. Photobiol. C: Photochem. Rev. 1 (2000) 1–21.
[11] A. Fujishima, K. Hashimoto, T. Watanabe, TiO_2 Photocatalysis: Fundamentals and Applications, Bkc, Tokyo, 1999.
[12] X. Chen, S.S. Mao, Titanium dioxide nanomaterials: synthesis, properties, modifications, and applications, Chem. Rev. 107 (2007) 2891–2959.
[13] X. Gao, I.E. Wachs, Titania–silica as catalysts: molecular structural characteristics and physico-chemical properties, Catal. Today 51 (1999) 233–254 (and references therein).
[14] H. Yamashita, S. Kawasaki, Y. Ichihashi, M. Harada, M. Takeuchi, M. Anpo, G. Stewart, M.A. Fox, C. Louis, M. Che, Characterization of titanium–silicon binary oxide catalysts prepared by the sol–gel method and their photocatalytic reactivity for the liquid-phase, J. Phys. Chem. B 102 (1998) 5870–5875.
[15] R. van Grieken, J. Aguado, M.J. López-Muñoz, J. Marugán, Synthesis of size-controlled silica-supported TiO_2 photocatalysts, J. Photochem. Photobiol. A: Chem. 148 (2002) 315–322.
[16] T. Tanaka, K. Teramura, T. Yamamoto, S. Takenaka, S. Yoshida, T. Funabiki, TiO_2/SiO_2 photocatalysts at low levels of loading: preparation, structure and photocatalysis, J. Photochem. Photobiol. A: Chem. 148 (2002) 277–281.
[17] B. Malinowska, J. Walendziewski, D. Robert, J.V. Weber, M. Stolarski, The study of photocatalytic activities of titania and titania–silica aerogels, Appl. Catal. B: Environ. 46 (2003) 441–451.
[18] K.Y. Jung, S.B. Park, Photoactivity of SiO_2/TiO_2 and ZrO_2/TiO_2 mixed oxides prepared by sol–gel method, Mater. Lett. 58 (2004) 2897–2900.

[19] Y. Chen, K. Wang, L. Lou, Photodegradation of dye pollutants on silica gel supported TiO_2 particles under visible light irradiation, J. Photochem. Photobiol. A: Chem. 163 (2004) 281–287.
[20] M. Jin, X. Zhang, A.V. Emeline, Z. Liu, D.A. Tryk, T. Murakami, A. Fujishima, Fibrous TiO_2–SiO_2 nanocomposite photocatalyst, Chem. Commun. (2006) 4483–4485.
[21] J. Aguado, R. van Grieken, M.J. López- Muñoz, J. Marugán, A comprehensive study of the synthesis, characterization and activity of TiO_2 and mixed TiO_2/SiO_2 photocatalysts, Appl. Catal. A: Gen. 312 (2006) 202–212.
[22] M. Zhang, T. An, J. Fu, G. Sheng, X. Wang, X. Hu, X. Ding, Photocatalytic degradation of mixed gaseous carbonyl compounds at low level on adsorptive TiO_2/SiO_2 photocatalyst using a fluidized bed reactor, Chemosphere 64 (2006) 421–423.
[23] J. Marugán, M.J. López-Muñoz, J. Aguado, R. van Grieken, On the comparison of photocatalysts activity: a novel procedure for the measurement of titania surface in TiO_2/SiO_2 materials, Catal. Today 124 (2007) 103–109.
[24] A. Maldotti, A. Molinari, R. Amadelli, E. Carbonell, H. Garcia, Photocatalytic activity of MCM-organized TiO_2 materials in the oxygenation of cyclohexane with molecular oxygen, Photochem. Photobiol. Sci. 7 (2008) 819–825.
[25] C. Hu, Y. Tang, J.C. Yu, P.K. Wong, Photocatalytic degradation of cationic blue X-GRL adsorbed on TiO_2/SiO_2 photocatalyst, Appl. Catal. B: Environ. 40 (2003) 131–140.
[26] J. Marugán, M.J. López-Muñoz, R. van Grieken, J. Aguado, Photocatalytic decolorization and mineralization of dyes with nanocrystalline TiO_2/SiO_2 materials, Ind. Eng. Chem. Res. 46 (2007) 7605–7610.
[27] C. Anderson, A.J. Bard, An improved photocatalyst of TiO_2/SiO_2 prepared by a sol–gel synthesis, J. Phys. Chem. 99 (1995) 9882–9885.
[28] Y. Xu, W. Zheng, W. Liu, Enhanced photocatalytic activity of supported TiO_2: dispersing effect of SiO_2, J. Photochem. Photobiol. A: Chem. 122 (1999) 57–60.
[29] Z. Ding, G.Q. Lu, P.F. Greenfield, Kinetic study on photocatalytic oxidation of phenol in water by silica-dispersed titania nanoparticles, J. Colloid Interface Sci. 232 (2000) 1–9.
[30] X. Fu, L.A. Clark, Q. Yang, M.A. Anderson, Enhanced photocatalytic performance of titania-based binary metal oxides: TiO_2/SiO_2 and TiO_2/ZrO_2, Environ. Sci. Technol. 30 (1996) 647–653.
[31] B. Bonelli, M. Cozzolino, R. Tesser, M. Di Serio, M. Piumetti, E. Garrone, E. Santacesaria, Study of the surface acidity of TiO_2/SiO_2 catalysts by means of FTIR measurements of CO and NH_3 adsorption, J. Catal. 246 (2007) 293–300.
[32] M. Cozzolino, M. Di Serio, R. Tesser, E. Santacesaria, Grafting of titanium alkoxides on high-surface SiO_2 support: an advanced technique for the preparation of nanostructured TiO_2/SiO_2 catalysts, Appl. Catal. A: Gen. 325 (2007) 256–262.
[33] P.K. Doolin, S. Alerasool, D.J. Zalewski, J.F. Hoffman, Acidity studies of titania-silica mixed oxides, Catal. Lett. 25 (1994) 209–223.
[34] A. Fernandez, A. Caballero, A.R. Gonzalez-Elipe, Size and support effects in the photoelectron spectra of small TiO_2 particles, Surf. Interf. Anal. 18 (1992) 392–396.
[35] S. Haukka, E. Lakomaa, A. Root, An IR and NMR study of the chemisorption of titanium tetrachloride on silica, J. Phys. Chem. 97 (1993) 5085–5094.
[36] M. Addamo, V. Augugliaro, A. Di Paola, E. García-López, V. Loddo, G. Marcì, L. Palmisano, Preparation and photoactivity of nanostructured TiO_2 particles obtained by hydrolysis of $TiCl_4$, Coll. Surf. A: Physicochem. Eng. Aspects 265 (2005) 23–31.
[37] D. Chen, A.K. Ray, Photodegradation kinetics of 4-nitrophenol in TiO_2 suspension, Water Res. 32 (1998) 3223–3234.
[38] N. Daneshvar, M.A. Behnajady, Y. Zorriyeh Asghar, Photooxidative degradation of 4-nitrophenol (4-NP) in UV/H_2O_2 process: influence of operational parameters and reaction mechanism, J. Hazard. Mater. 139 (2007) 275–279.
[39] R. Amadelli, L. Samiolo, Concrete containing TiO_2: an overview of photocatalytic NO_x abatement, in: P. Baglioni, L. Cassar (Eds.), Photocatalysis, Environment and Construction Materials–TDP 2007, RILEM Publication SARL, Bagneux, 2007, pp. 155–162.
[40] V. Desauziers, Traceability of pollutant measurements for ambient air monitoring, Trends Anal. Chem. 23 (2004) 252–260.
[41] F.P. Koffyberg, K. Dwight, A. Wold, Interband transitions of semiconducting oxides determined from photoelectrolysis spectra, Solid State Commun. 30 (1979) 433–437.
[42] Y.I. Kim, S.J. Atherton, E.S. Brigham, T.E. Mallouk, Sensitized layered metal oxide semiconductor particles for photochemical hydrogen evolution from nonsacrificial electron donors, J. Phys. Chem. 97 (1993) 11802–11810.